

■ Aryl Methanol Oxidation



Cerium-Complex-Catalyzed Oxidation of Aryl Methanols under Atmospheric Pressure of Dioxygen and Its Mechanism through a Side-On μ -Peroxo Dicerium(IV) Complex

Mitali Paul,^[a] Satoru Shirase,^[a] Yuma Morimoto,^[b] Laurent Mathey,^[a] Balasubramanian Murugesapandian,^[a] Shinji Tanaka,^[a] Shinobu Itoh,^[b] Hayato Tsurugi,^{*[a]} and Kazushi Mashima^{*[a]}

Abstract: A new Ce^{IV} complex [Ce{NH(CH₂CH₂N=CHC₆H₂-3,5-(tBu)₂-2-O)₂}(NO₃)₂] (1), bearing a dianionic pentadentate ligand with an N₃O₂ donor set, has been prepared by treating (NH₄)₂Ce(NO₃)₆ with the sodium salt of ligand L1. Complex 1 in the presence of TEMPO and 4 Å molecular sieves (MS4A) has been found to serve as a catalyst for the oxidation of arylmethanols using dioxygen as an oxidant. We propose an oxidation mechanism based on the isolation and reactivity study of a trivalent cerium complex [Ce{NH(CH₂CH₂N=CHC₆H₂-3,5-(tBu)₂-2-O)₂}(NO₃)(THF)] (2), its

side-on μ -O₂ adduct [Ce{NH(CH₂CH₂N=CHC₆H₂-3,5-(tBu)₂-2-O)₂}(NO₃)₂](μ - η^2 : η^2 -O₂) (3), and the hydroxo-bridged Ce^{IV} complex [Ce{NH(CH₂CH₂N=CHC₆H₂-3,5-(tBu)₂-2-O)₂}(NO₃)₂](μ -OH)₂ (4) as key intermediates during the catalytic cycle. Complex 2 was synthesized by reduction of 1 with 2,5-dimethyl-1,4-bis(trimethylsilyl)-1,4-diazacyclohexadiene. Bubbling O₂ into a solution of 2 resulted in formation of the peroxo complex 3. This provides the first direct evidence for cerium-catalyzed oxidation of alcohols under an O₂ atmosphere.

Introduction

Most lanthanide elements favor the +3 oxidation state, although some, such as Sm, Eu, and Yb, adopt the +2 oxidation state. A unique exception, however, is Ce because of the relative accessibility of two stable oxidation states, +3 and +4, and this redox couple can be utilized for many chemical redox processes.^[1] In fact, Ce^{IV}-based compounds, such as cerium ammonium nitrate, (NH₄)₂Ce(NO₃)₆ (CAN), are widely used as versatile oxidants in organic transformations, bioinorganic reactions, and electron-transfer chemistry,^[2] though (NH₄)₂Ce(NO₃)₆ often serves only as a stoichiometric oxidant. In addition to several transition metal complexes with Cu, Co, Fe, Ru, Mn, and V, which serve as catalysts for aerobic oxidation of alcohols in combination with a stable radical such as 2,2,6,6-tetramethylpiperidine 1-oxyl (TEMPO), the preparation of discrete cerium compounds capable of catalytically oxidizing organic compounds with dioxygen as a terminal oxidant has attracted

much interest.^[3-5] Three examples of side-on μ -peroxo dicerium(IV) complexes have recently been reported and structurally characterized. Lappert et al. described a μ -peroxo complex of homoleptic cerium amide **A**,^[6a] Leung et al. described doubly μ -peroxo-bridged Ce^{IV} complex **B** supported by a monoanionic imidodiphosphinate ligand,^[6b] and Reglinski et al. described a μ -peroxo Ce^{IV} complex **C** supported by a tripodal phenoxyamine-based ligand (Figure 1).^[6c] The catalytic performances

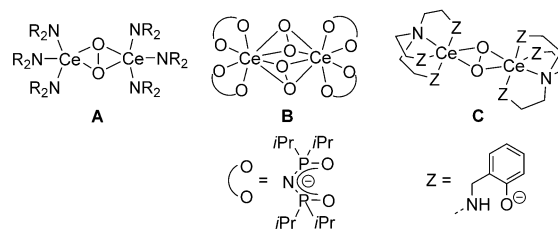


Figure 1. Peroxo-bridged dinuclear cerium complexes reported by other groups.

and fundamental reactivities of these μ -peroxo complexes for oxidation reactions, however, were not investigated. In this context, we report herein the first direct evidence for cerium-catalyzed oxidation of alcohols under O₂ in combination with TEMPO and 4 Å molecular sieves (MS4A). A dinuclear peroxo-cerium complex containing a Ce₂(μ -O₂) core has been isolated and structurally characterized as a key intermediate for the alcohol oxidation process, in which a mononuclear Ce^{IV} complex

[a] M. Paul, S. Shirase, Dr. L. Mathey, Dr. B. Murugesapandian, Dr. S. Tanaka, Prof. Dr. H. Tsurugi, Prof. Dr. K. Mashima
Department of Chemistry, Graduate School of Engineering Science
Osaka University, Toyonaka, Osaka 560-8531 (Japan)
E-mail: mashima@chem.es.osaka-u.ac.jp
tsurugi@chem.es.osaka-u.ac.jp

[b] Dr. Y. Morimoto, Prof. Dr. S. Itoh
Department of Material and Life Science, Graduate School of Engineering,
Osaka University, Suita, Osaka 565-0871 (Japan)

Supporting information for this article is available on the WWW under
<http://dx.doi.org/10.1002/chem.201503846>.

bearing a Schiff-base-type ligand served as the catalyst. Furthermore, we have successfully isolated and characterized a mononuclear Ce^{III} species as well as a (OH)₂-bridged dinuclear Ce^{IV} species.

Results and Discussion

Reaction of (NH₄)₂Ce(NO₃)₆ with the disodium compound NH(CH₂CH₂N=CHC₆H₂-3,5-(*t*Bu)₂-2-ONa)₂ (**L1**), prepared by condensation of 3,5-bis(*tert*-butyl)salicylaldehyde and diethylenetriamine followed by deprotonation using NaH, afforded the mononuclear Ce^{IV} complex **1** [Eq. (1)]. The ¹H NMR spectrum of **1** in CDCl₃ displays a pattern befitting a symmetric molecule, with three singlet resonances at δ = 8.61, 7.59, and 7.13 ppm attributable to an imine proton and two aromatic protons, two singlets at δ = 1.31 and 1.50 ppm attributable to two magnetically non-equivalent *t*Bu groups, and four broad multiplets attributable to the adjacent -CH₂CH₂- methylene protons. The UV/Vis spectrum of **1** in CH₃CN features a broad absorption at λ_{max} = 594 cm⁻¹, corresponding to a ligand-to-metal charge-transfer band from the ligand π orbital to the vacant Ce 4f orbital, which is characteristic of Ce^{IV} complexes (Figure 2).^[7]

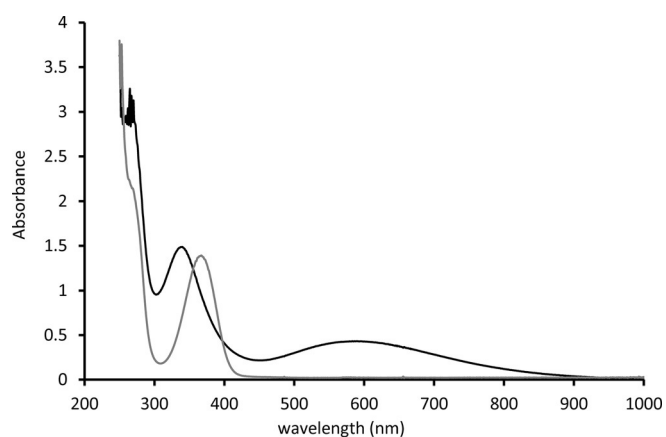


Figure 2. UV/Vis spectra of cerium complexes **1** and **2** in CH₃CN: complex **1** (black line) and complex **2** (gray line).

Cyclic voltammetry of **1** in CH₃CN containing [nBu₄N]PF₆ displays a reversible reduction wave at E_{1/2} = -0.493 V (vs Cp₂Fe), negatively shifted with respect to the potential of CAN, presumably due to ligation of the electron-rich ligand **L1** to the Ce^{IV} centre of **1**.^[7c,8] The crystal structure of complex **1** was determined by X-ray diffraction analysis (Figure 3). The cerium atom of **1** occupies a distorted nine-coordinated geometry, being surrounded by three nitrogen atoms and two oxygen atoms in a distorted penta-coordinated equatorial plane, along with further coordination at both apical sites by two chelating NO₃ anions. The dihedral angle (58.3°) between the two phenoxy rings of the ligand indicates a deformation of the penta-coordinated plane due to steric repulsion between the two *t*Bu groups attached at the *ortho* positions of the respective rings.

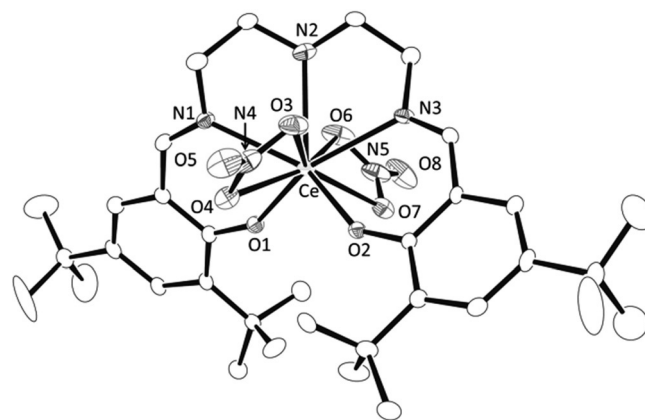
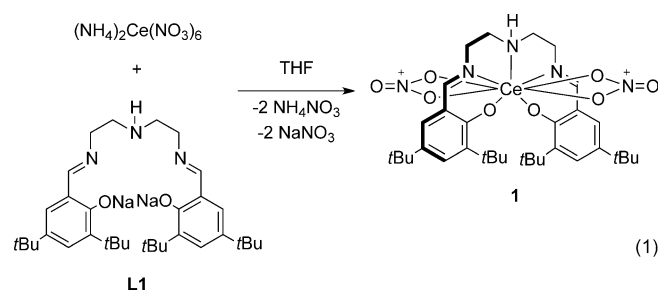


Figure 3. Molecular structure of complex **1**. All hydrogen atoms are omitted for clarity. Selected bond distances (Å) and angles (degree): Ce–N(1) 2.569(8), Ce–N(2) 2.638(8), Ce–N(3) 2.531(8), Ce–O(1) 2.127(7), Ce–O(2) 2.150(6), Ce–O(3) 2.517(9), Ce–O(4) 2.523(8), Ce–O(6) 2.520(8), Ce–O(7) 2.508(8); N1–Ce–N2 63.0(3), N2–Ce–N3 65.8(3), O1–Ce–O2 103.2(3), O1–Ce–N1 72.7(3), O2–Ce–N3 70.6(3).



Selective oxidation of alcohols to aldehydes under O₂ atmosphere without any over-oxidation of the organic compounds is a highly desirable reaction in organic synthesis.^[9] Complex **1** was found to serve as a catalyst for the selective oxidation of arylmethanols (Table 1). When we oxidized 4-methylbenzyl alcohol using **1** (5 mol%) in the presence of MS4A with TEMPO (10 mol%) in CH₃CN under O₂ at atmospheric pressure in

Table 1. Oxidation of 4-methylbenzyl alcohol catalyzed by **1**/TEMPO/MS4A under O₂ atmosphere.^[a]

Entry	Cat. [mol%]	TEMPO [mol%]	Yield ^[a] [%]
1	5	10	83
2	5	–	33
3 ^[b]	5	10	69
4 ^[c]	5	10	10
5	5	5	51
6	–	10	2
7 ^[d]	5	10	n.d.

[a] Yields were calculated by ¹H NMR. [b] MS4A was not added. [c] NEt₃ (10 mol%) was used as an additive. [d] Reaction under argon atmosphere.

a closed vessel for 20 h, the corresponding oxidized product, 4-methylbenzaldehyde, was obtained in 83% yield (entry 1). In contrast, the yield of the reaction without TEMPO was only 33% (entry 2). In the absence of MS4A, the yield of the product was also decreased, presumably because MS4A served as a heterogeneous base rather than absorbing water (entry 3).^[10] On the other hand, the addition of an organic base such as NEt₃ in the absence of MS4A resulted in a lower yield (entry 4). Reducing the amount of TEMPO to 5 mol% decreased the product yield (entry 5). Furthermore, omission of either complex **1** or O₂ resulted in only a trace amount of the aldehyde, indicating that all four components of **1**, O₂, MS4A, and TEMPO were necessary in this catalytic oxidation (entries 6 and 7). When the catalytic reaction was conducted in hexane, toluene, THF, or chloroform, it was less effective than when conducted in CH₃CN.

Once the optimized catalytic conditions had been determined, we oxidized a variety of benzyl alcohols bearing electron-donating and -withdrawing groups at their *ortho*, *meta*, and *para* positions to the corresponding aldehydes (Table 2). We increased the temperature and reaction time to improve

Table 2. Oxidation of benzyl alcohol derivatives by **1**/TEMPO/MS4A under O₂ atmosphere.^[a]

Entry	Substrate	R	Yield [%] ^[a]
1		R = OMe	92
2		R = Me	85
3		R = H	81
4		R = Br	71 (94) ^[b]
5		R = CF ₃	62 (90) ^[b]
6		R = OMe	65
7		R = Me	67
8		R = CF ₃	22 (70) ^[b]
9		R = OMe	72
10		R = Me	79
11		R = CF ₃	40 (87) ^[b]

[a] Yields were calculated by ¹H NMR. [b] 10 mol% catalyst was used.

the product yields for a series of substrates. *para*-Substituted benzyl alcohols bearing an electron-donating group such as methoxy or methyl afforded the corresponding aldehydes in good yields (entries 1 and 2). Benzyl alcohols bearing electron-withdrawing substituents gave lower product yields, but increasing the amount of catalyst to 10 mol% led to the oxidized products in up to 94% yield (entries 4 and 5). Benzyl alcohol derivatives bearing a substituent at the *ortho* position reacted more slowly due to steric congestion (entries 6–8). For *meta*-substituted substrates, the corresponding aldehydes were obtained in moderate yields (entries 9–11).

Moreover, the electronic effects on the catalytic reaction were systematically probed by comparing the relative reaction rates with electronically varied substituents (X = OMe, Me, H,

Br, CF₃) in CH₃CN at 85 °C for 10 h. In these experiments, two substrates, benzyl alcohol and a *para*-substituted derivative, were added to the same reaction vessel, and the progress of the reactions was monitored by ¹H NMR spectroscopy. The observed reaction rates correlated reasonably well to the Hammett σ_p parameters, providing a ρ value of -0.77 ,^[11] which implies radical intermediate formation at the benzylic position of the substrate in the transition state for the oxidation process (see below).

Next, we performed control experiments to clarify the reaction mechanism. We first examined the reaction of complex **1** and 4-methylbenzyl alcohol in CH₃CN at 80 °C. In the ESI mass spectrum of the reaction mixture, signals for [LCe^{III}(NO₃)(OCH₂Ar)]⁻ and [LCe^{IV}(NO₃)₂(OCH₂Ar)]⁻ were detected in negative-ion mode.^[11] The one-electron-reduced Ce^{III} species was formed under the ESI-MS conditions for negative-ion signals. We further conducted UV/Vis measurements. When a solution of complex **1** (5 mol%), TEMPO (10 mol%), and 4-methylbenzyl alcohol in CH₃CN was heated at 80 °C for 32 h under argon atmosphere, we observed a transition of the absorption spectrum. Bands at λ_{\max} = 340 and 576 nm attributable to complex **1** slowly decreased, with a concomitant increase in a band at λ_{\max} = 370 nm (Figure 4). This behavior

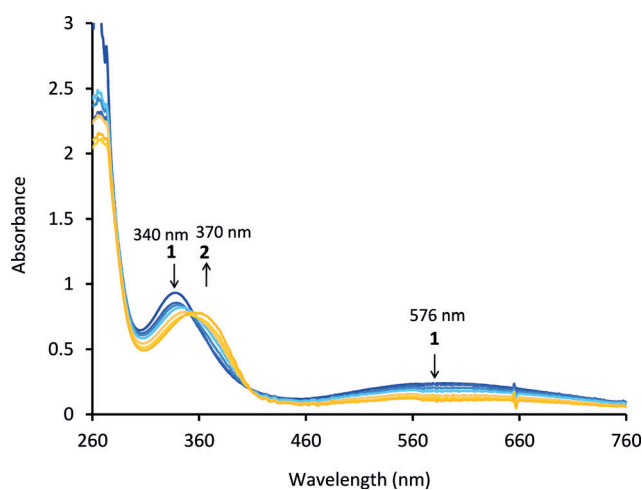


Figure 4. Time-dependent UV/Vis spectra of a mixture of complex **1**, TEMPO, and 4-methylbenzyl alcohol in CH₃CN under argon atmosphere.

could be ascribed to the reduction of Ce^{IV} to Ce^{III} in the reaction mixture, based on the spectral data of the isolated Ce^{IV} and Ce^{III} species (see below). We also monitored the reduction of **1** by ¹H NMR spectroscopy. When an analogous reaction mixture in CD₃CN was heated at 80 °C under argon atmosphere for 6 h, highly downfield- and upfield-shifted signals were observed due to paramagnetic species, clearly suggesting the formation of a paramagnetic Ce^{III} complex.^[11]

The detection of a Ce^{III} species by spectral measurements prompted us to attempt its isolation to gain further insight into the mechanism. Treatment of **1** with 2,5-dimethyl-1,4-bis-(trimethylsilyl)-1,4-diazacyclohexadiene^[12] gave a Ce^{III} complex, [(L)Ce(NO₃)(THF)] (**2**), in 49% isolated yield [Eq. (2)]. Because of

the paramagnetic nature of complex **2**, the resonances in the ^1H NMR spectrum were highly shifted both upfield and downfield.^[11] Signals at $\delta = 4.37$ and -4.22 ppm could be attributed to the two *t*Bu groups, based on their relative intensities. The UV/Vis spectrum of **2** in CH_3CN displayed only a ligand $\pi\text{-}\pi^*$ transition centred at $\lambda_{\text{max}} = 370$ nm (Figure 2, gray line), in good accordance with the spectrum observed for in situ generated **2** under argon atmosphere, as shown in Figure 4.^[7,11]

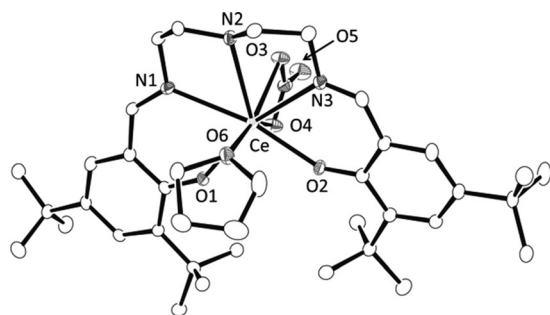
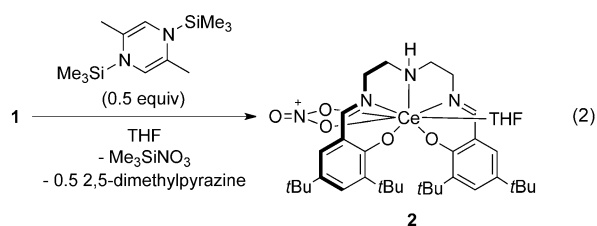


Figure 5. Molecular structure of complex **2**. All hydrogen atoms are omitted for clarity. Selected bond lengths (Å) and angles (degree): Ce–N(1) 2.716(5), Ce–O(1) 2.285(4), Ce–N(2) 2.674(4), Ce–O(2) 2.298(3), Ce–N(3) 2.740(5), Ce–O(3) 2.613(4), Ce–O(4) 2.585(5); N1–Ce–N2 62.11(12), N2–Ce–N3 62.86(14), O1–Ce–N1 67.11(13), O1–Ce–O2 99.02(12), O2–Ce–N3 68.65(12).

Figure 5 shows an ORTEP drawing of **2**, clearly indicating that it is a Ce^{III} compound, as one nitrate ligand of **1** was replaced by a THF ligand. The Ce–O(THF) bond length is 2.526(4) Å and the bond lengths between the cerium atom and two oxygen atoms of the nitrate ligand [2.585(5)–2.613(4) Å] are significantly elongated compared to those in **1** [2.507(8)–2.523(8) Å]. The Ce–O(phenoxy) bond lengths are longer by about 0.13 Å than those in complex **1** due to the larger ionic radius of Ce^{III} (1.01 Å) than that of Ce^{IV} (0.87 Å),^[13] leading to a less deformed chelating ligand compared with that in **1**.



With the Ce^{III} complex **2** in hand, we examined the effects of bubbling O_2 through a dilute solution (0.125 mM) of **2** in CH_3CN at -40°C , which induced a very rapid color change from yellow to violet within a few seconds. Time-resolved UV/Vis spectrophotometry in CH_3CN at -40°C showed the disappearance of complex **2** with the appearance of new absorptions at 340 and 529 nm due to Ce^{IV} complex **3**. The absorption at 529 nm could be attributed to a ligand-to-metal charge transfer in **3**, similar to that in complex **1** (purple line in Figure 6, $\lambda_{\text{max}} = 340, 529$ nm). During this transition, two isosbestic points at 353 and 393 nm were observed. Formation of

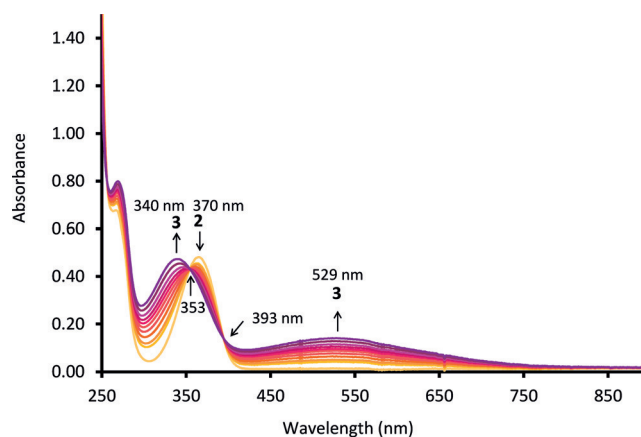


Figure 6. Time-dependent UV/Vis spectra obtained upon mixing a solution of Ce^{III} complex **2** (0.040 mM) in CH_3CN and O_2 at -40°C in a 10 mm quartz cell.

the Ce^{IV} peroxy complex **3** was confirmed by ESI-MS analysis of the purple solution, whereby a signal due to $[\mathbf{3}\cdot(\text{NO}_3)]^-$ was observed in negative-ion mode.^[11]

When O_2 was bubbled into a solution of **2** in CH_3CN at -30°C under high concentration conditions (17.7 mM), spontaneous crystallization of **3** proceeded to give sparingly soluble needle-shaped dark-violet microcrystals [Eq. (3)]. The overall structure of **3**, in which two cerium atoms are bridged by the $\mu\text{-}\eta^2\text{:}\eta^2\text{-peroxy}$ ligand, is shown in Figure 7. The length of the O–O bond in the peroxy moiety was determined as 1.483(8) Å, a value within the typical range of oxygen-oxygen single bonds observed in dinuclear peroxy-bridged complexes of Ce and other lanthanides.^[6,14] The peroxy ligand asymmetrically binds to two cerium atoms (Ce–O(peroxy) 2.237–2.298 Å) to reduce the steric repulsion between the *tert*-butyl groups. The dihedral angles of the two phenoxy rings are smaller (31.5° and 34.4°) than that in complex **1** due to the restricted confor-

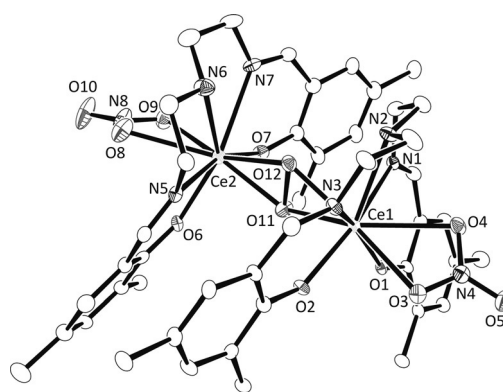
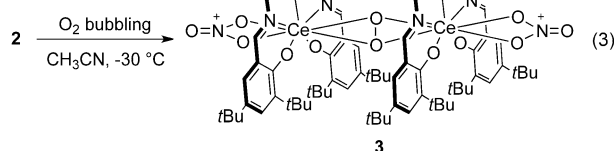
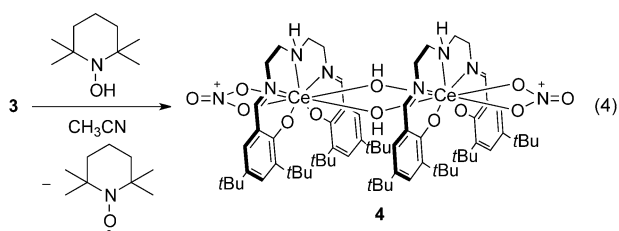


Figure 7. Molecular structure of complex **3**. All hydrogen atoms, methyl groups, and acetonitrile ligands are omitted for clarity. Selected bond lengths (Å) and angles (degree): O(11)–O(12) 1.483(8), Ce(1)–O(1) 2.168(5), Ce(1)–O(2) 2.170(5), Ce(1)–O(3) 2.520(6), Ce(1)–O(4) 2.594(6), Ce(1)–O(11) 2.298(6), Ce(1)–O(12) 2.257(6), Ce(2)–O(6) 2.185(5), Ce(2)–O(7) 2.147(5), Ce(2)–O(8) 2.551(7), Ce(2)–O(9) 2.621(8), Ce(2)–O(11) 2.291(6), Ce(2)–O(12) 2.237(6); N1–Ce1–N2 65.4(2), N2–Ce1–N3 62.1(2), N1–Ce1–N3 127.2(2), Ce1–O11–Ce2 138.3(3), Ce1–O12–Ce2 145.2(3).

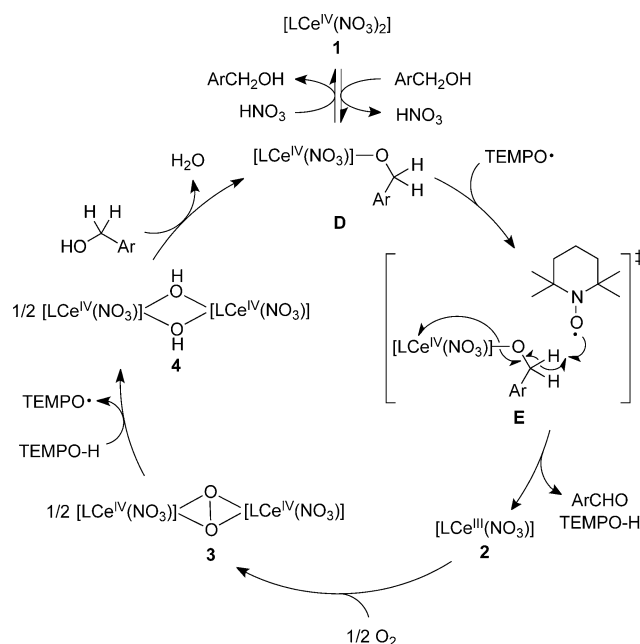
mation in the dimeric structure. The Ce–O(phenoxy) bond lengths are essentially the same as those in complex **1**, but 0.11–0.15 Å shorter than those in complex **2**, indicating the formation of a Ce^{IV} centre in complex **3**. In situ reduction of the Ce^{IV} complex **1** with alcohols and TEMPO, giving the Ce^{III} species, as well as O₂-induced oxidation of the Ce^{III} species, clearly indicated that the dinuclear peroxy species **3** was involved in the catalytic alcohol oxidation.



Although the solution of **3** in acetonitrile was relatively stable to water and benzyl alcohol at room temperature, **3** reacted with TEMPO-H to produce a brown-colored solution of hydroxo-bridged cerium complex **4** [Eq. (4)]. In the ¹H NMR spectrum, a singlet at δ = 8.68 ppm and two doublets at δ = 7.50 and 7.29 ppm with a long-range coupling constant (⁴J_{H-H} = 2.4 Hz) could be attributed to the imine and aromatic protons, respectively. ESI-MS analysis of **4** was consistent with the formation of a bis(hydroxyl)-bridged structure.^[11] Accordingly, the dioxygen activation proceeded through formation of the peroxy intermediate **3**, and subsequent reaction with TEMPO-H in the reaction medium afforded hydroxo-bridged cerium complex **4**. UV/Vis transition in the course of the reaction according to Equation (4) clearly indicated consumption of the peroxy complex **3**.^[11]



Based on the above findings concerning the reactivity of the Ce^{IV} complex **1** toward the substrate and TEMPO (Figure 4), and of Ce^{III} complex **2** toward O₂ and TEMPO-H [Eq. (4)], we propose a catalytic cycle for the alcohol oxidation as shown in Scheme 1. In the first stage, in the presence of alcohol, Ce^{IV} species **1** is converted to arylmethoxycerium(IV) **D** with the generation of HNO₃. The cerium species **D** was detected by ESI-MS measurement.^[11] The related arylmethoxycerium and -lanthanide complexes are rare, and reported to adopt a homoleptic dimer form.^[15] The importance of MS4A is presumably due to trapping of the in situ generated HNO₃ at this stage, as otherwise protonation of species **D** by HNO₃ would proceed to regenerate the Ce^{IV} complex **1**. By reacting with TEMPO, Ce^{IV}



Scheme 1. Proposed catalytic cycle for cerium-catalyzed alcohol oxidation (L = Schiff-base N₃O₂ ligand).

species **D** is reduced to form Ce^{III} complex **2** along with TEMPO-H and aldehydes, which corresponds to the arylmethanol oxidation in this catalytic cycle. The small negative σ_p value in the Hammett analysis is consistent with transition state **E**, in which a carbon radical is generated at the benzylic position. The next step is oxidation of the Ce^{III} complex **2** by O₂ to form side-on μ -peroxy dicerium(IV) complex **3**, which was clearly confirmed by the isolation and structural characterization of such a peroxy species. When isolated Ce^{III} complex **2** was used as the catalyst with TEMPO-H, the catalytic activity for the alcohol oxidation was almost the same as that with complex **1**/TEMPO. Complex **3** then reacts with TEMPO-H to produce the hydroxo-bridged cerium complex **4** along with regeneration of TEMPO. Finally, alcoholysis of **4** by arylmethanol produces cerium complex **1**, as also supported by ESI-MS measurement.^[11]

Conclusion

We have demonstrated the synthesis and characterization of a mononuclear Ce^{IV} complex **1** bearing a Schiff-base-type dianionic pentadentate ligand. Complex **1** served as an effective catalyst for the aerobic oxidation of arylmethanols in the presence of TEMPO, MS4A, and O₂. We propose a mechanism for the catalytic reaction based on experimental evidence that the Ce^{III} complex **2**, derived from reduction of **1** with arylmethanol and TEMPO, reacted with O₂ to give side-on μ -peroxy dicerium(IV) complex **3**. In addition, treatment of **3** with TEMPO-H produced the hydroxo-bridged dinuclear complex **4**. The negative and small ρ value obtained in a Hammett analysis suggested the transition state **E**, in which a benzylic carbon radical is formed during substrate oxidation.

Experimental Section

General: All manipulations involving air- and moisture-sensitive organometallic compounds were performed under argon using standard Schlenk techniques or an argon-filled glovebox. Ligand L1 and 2,5-dimethyl-1,4-bis(trimethylsilyl)-1,4-diaza-2,5-cyclohexadiene were prepared according to the literature.^[16] $(\text{NH}_4)_2\text{Ce}(\text{NO}_3)_6$ was purchased from Sigma-Aldrich and used as received. Anhydrous hexane, toluene, THF, and dichloromethane were purchased from Kanto Chemical, and were further purified by passage through activated alumina under positive argon pressure as described by Grubbs et al.^[17] MS4A was purchased from Nacal Tesque, dried at 300 °C for 2 days, and then stored inside a glovebox. CD_3CN was distilled over CaH_2 and degassed before use. ^1H NMR (400 MHz) and ^{13}C NMR (100 MHz) spectra were measured on Bruker Avance III-400 spectrometers. Electrochemical measurements were carried out in a glovebox at room temperature, using a 0.1 M solution of $[\text{tBu}_4\text{N}][\text{PF}_6]$ in CH_3CN as the supporting electrolyte, an Ag wire as the reference electrode, and a Pt wire as the counter electrode, at a scan rate of 100 mVs^{-1} . Infrared spectra were recorded on a JASCO FT/IR-230 spectrometer from samples in KBr pellets. Typically, 32 scans were accumulated for each spectrum (resolution 4 cm^{-1}). UV/Vis spectra were measured using an Agilent 8453 UV/Vis spectroscopy system. All melting points were measured for samples in sealed tubes under argon atmosphere on a Büchi M-565 melting point apparatus (1 °C min^{-1}). Elemental analyses were determined on a Perkin-Elmer 2400 analyzer at the Faculty of Engineering Science, Osaka University.

Preparation of Ce^{IV} complex 1: A solution of the disodium salt of ligand L1, $\{\text{NH}(\text{CH}_2\text{CH}_2\text{N}=\text{CHC}_6\text{H}_2-3,5-\text{tBu}_2-2\text{-ONa})_2\}$ (250 mg, 4.31×10^{-1} mmol), in THF (20 mL) was added to a solution of $(\text{NH}_4)_2\text{Ce}(\text{NO}_3)_6$ (236 mg, 4.30×10^{-1} mmol) in THF (30 mL) via a cannula at room temperature under Ar atmosphere. After stirring for 2 h, the reaction mixture had turned blue and a white precipitate had separated. All volatiles were removed in vacuo, and then the blue product was extracted with toluene (2×15 mL). The solvent was evaporated, and the product was isolated as a blue powder in 76% yield (254 mg). Single crystals suitable for X-ray diffraction study were obtained by cooling a saturated solution in toluene/hexane. The cyclic voltammogram of complex 1 is shown in Figure S5, which features a reversible $\text{Ce}^{\text{IV}}/\text{Ce}^{\text{III}}$ wave. M.p. 215 °C (decomp.); ^1H NMR (400 MHz, CDCl_3 , 30 °C): δ = 8.61 (s, 2H; N=CH), 7.59 (s, 2H; Ar), 7.13 (s, 2H; Ar), 4.17 (brt, 2H; CHH), 3.98 (brd, 2H; CHH), 3.42–3.52 (brm, 2H; CHH), 3.19–3.33 (brm, 2H; CHH), 3.05–3.16 (brm, 1H; N-H), 1.50 (s, 18H; tBu), 1.30 ppm (s, 18H; tBu); $^{13}\text{C}\{^1\text{H}\}$ NMR (100 MHz, CDCl_3 , 30 °C): δ = 167.7 (N=CH), 166.3 (C-O of Ar), 143.2 (C-C(CH_3)₃ of Ar), 135.2 (C-C(CH_3)₃ of Ar), 129.8 (C-H of Ar), 129.4 (C-H of Ar), 127.3 (C-CH=N of Ar), 62.1 (CH_2 -N=CH), 50.6 (CH_2 - CH_2 -NH), 35.2 (C(CH_3)₃), 33.9 (C(CH_3)₃), 31.9 (C(CH_3)₃), 30.8 ppm (C(CH_3)₃); IR (KBr): $\tilde{\nu}$ = 3230 (w), 2960 (s), 2868 (m), 1620 (s), 1556 (m), 1512 (vs), 1467 (s), 1436 (s), 1412 (m), 1392 (m), 1362 (w), 1332 (w), 1262 (vs), 1201 (w), 1175 (w), 1100 (m), 1020 (s), 875 (w), 836 (s), 810 (s), 775 (w), 747 (w), 734 (m), 528 (m), 450 cm^{-1} (w); UV/Vis (THF): λ_{max} (ϵ) = 340 (1.19×10^4), 594 nm ($3.48 \times 10^3 \text{ dm}^3 \text{ mol}^{-1} \text{ cm}^{-1}$); ESI-MS (negative mode) $[(\text{C}_{34}\text{H}_{51}\text{N}_3\text{O}_2)(\text{NO}_3)_2\text{Ce}]^-$: m/z 797. Despite several attempts, we were unable to obtain reproducible elemental analysis data for this complex. The ^1H and ^{13}C NMR spectra are shown in Figure S3.

Preparation of Ce^{III} complex 2: A solution of 2,5-dimethyl-1,4-bis(trimethylsilyl)-1,4-diaza-2,5-cyclohexadiene (32.0 mg, 1.20×10^{-1} mmol) in toluene (5 mL) was added to a solution of 1 (200 mg, 2.50×10^{-1} mmol) in toluene (5 mL) at room temperature inside a glovebox. The color of the solution immediately

changed from dark-blue to yellow. The reaction mixture was stirred for 10 min, and then the solvent was evaporated. The complex was crystallized from THF containing a few drops of hexane at room temperature to give yellow crystals of 2 in 49% yield (100 mg, 0.120 mmol). M.p. 210 °C (decomp.); ^1H NMR (400 MHz, CD_3CN , 30 °C): δ = 31.88, 18.52, 11.43, 7.49, 4.37 (s, 18H; tBu), -0.49, -4.20 (s, 18H; tBu), -4.48, -14.75 ppm; IR (KBr): $\tilde{\nu}$ = 3249 (m), 2955 (s), 1623 (s), 1537 (s), 1412 (s), 1354 (m), 1308 (s), 1201 (m), 1167 (s), 1141 (w), 1068 (m), 1024 (s), 952 (w), 912 (w), 872 (m), 835 (s), 810 (m), 787 (m), 744 (s), 703 (w), 640 (w), 521 (m), 439 cm^{-1} (m); UV/Vis (THF): λ_{max} (ϵ) = 367 nm ($1.12 \times 10^4 \text{ dm}^3 \text{ mol}^{-1} \text{ cm}^{-1}$); elemental analysis calcd (%) for $\text{C}_{38}\text{H}_{59}\text{CeN}_4\text{O}_6$ (808.03): C 56.49, H 7.36, N 6.93; found: C 56.75, H 7.49, N 6.62.

Preparation of complex 3: Complex 2 (100 mg, 1.24 mmol) was placed in a pre-dried Schlenk flask inside a glovebox and dry CH_3CN (7.0 mL) was added to prepare a 17.7 mM solution. The Schlenk flask was removed from the glovebox and the argon above the solution was replaced by dry oxygen. The color of the solution immediately changed from yellow to dark-violet. It was left to stand at room temperature for 8 h, giving nice violet needle-shaped crystals. The solvent was decanted off to give dark-violet crystals of 3 in 73% yield. IR (KBr): $\tilde{\nu}$ = 3254 (w), 2956 (s), 2866 (m), 1627 (s), 1553 (m), 1507 (s), 1435 (s), 1412 (s), 1390 (m), 1360 (m), 1331 (w), 1255 (s), 1201 (m), 1172 (m), 1141 (w), 1068 (w), 1022 (w), 980 (w), 928 (w), 912 (w), 873 (w), 834 (m), 809 (m), 778 (m), 745 (m), 642 (w), 576 (m), 524 cm^{-1} (w); UV/Vis (THF): λ_{max} (ϵ) = 339 nm (1.14×10^4), 529 nm ($3.37 \times 10^3 \text{ dm}^3 \text{ mol}^{-1} \text{ cm}^{-1}$); elemental analysis calcd (%) for $\text{C}_{68}\text{H}_{102}\text{Ce}_2\text{N}_8\text{O}_{12}$ (1502.57): C 54.31, H 6.84, N 7.45; found: C 54.33, H 6.68, N 7.37.

Preparation of hydroxo-bridged Ce^{IV} complex 4: TEMPO-H (9.8 mg, 3.05×10^{-2} mmol) was added to a solution of complex 2 (50.0 mg, 3.09×10^{-2} mmol) in CH_3CN (12.5 mL) under argon. Dioxxygen was then bubbled into the solution and the reaction mixture was left to stand for 3 h. The color changed from yellow to red-brown as complex 4 was quantitatively formed (see Figures S7 and S8). It was isolated in 82% yield. M.p. 249 °C (decomp.); ^1H NMR (400 MHz, CD_3CN , 30 °C): δ = 8.68 (s, 2H; N=CH), 7.50 (s, 2H; Ar), 7.29 (s, 2H; Ar), 4.16–4.08 (brm, 1H; N-H), 4.00–3.91 (brm, 4H; CH_2), 3.88–3.80 (brm, 4H; CH_2), 1.37 (s, 18H; tBu), 1.31 ppm (s, 18H; tBu); IR (KBr): $\tilde{\nu}$ = 3369 (w), 3280 (w), 3092 (m), 2960 (w), 2604 (w), 2259 (vs), 2115 (w), 1943 (w), 1943 (w), 1883 (w), 1391 (w), 1192 (m), 1101 (m), 1038 (s), 889 (m), 837 (s), 824 (s), 779 (s), 749 (s), 740 (s), 728 (s), 715 (s), 705 (s), 672 (s), 653 cm^{-1} (s); UV/Vis (THF): λ_{max} (ϵ) = 329 (1.70×10^4), 476 nm ($5.63 \times 10^3 \text{ dm}^3 \text{ mol}^{-1} \text{ cm}^{-1}$); ESI-MS (negative mode) $[(\text{C}_{34}\text{H}_{51}\text{N}_3\text{O}_2)_2(\text{NO}_3)_2\text{Ce}_2(\text{OH})_2(\text{CH}_3\text{CN})(\text{OH})]^-$: m/z 1562. Despite several attempts, we were unable to obtain reproducible elemental analysis data for this complex. Because of the low solubility of complex 4, no ^{13}C NMR spectral data could be obtained.

Catalytic alcohol oxidation: The typical procedure for alcohol oxidation was as follows. The requisite alcohol (2.04×10^{-1} mmol), complex 1 (0.10×10^{-1} mmol, 5 mol%), MS4A (40 mg), and TEMPO (0.19×10^{-1} mmol, 10 mol%) were added to a J. Young Schlenk tube (30 mL) under argon. CH_3CN (1 mL) was added by means of a syringe, and then the argon inside of the tube was replaced by O_2 at atmospheric pressure. After heating the closed reaction vessel at 85 °C for 28 h, it was allowed to cool to room temperature and a portion of the reaction mixture was diluted with CD_3CN for ^1H NMR spectroscopic analysis. The yield was determined from the relative intensities of the signals of the product and the starting compound. A typical ^1H NMR spectrum is shown in Figure S1.

Time-dependent UV/Vis spectra

Reduction process: A 0.2 cm UV cell containing 0.39 mM complex **1**, 0.79 mM TEMPO, and 7.89 mM 4-methylbenzyl alcohol was placed in a UV/Vis spectrophotometer. The UV cell was heated at 80 °C for 32 h under argon, and the progress of the reaction was monitored at intervals of 1 h by UV/Vis spectrophotometry (Figure 4).

Reaction of complex **2 with dioxygen:** A 0.12 mM solution of complex **2** in CH₃CN was placed in a 1 cm UV cell fitted with a rubber septum. O₂ gas was bubbled through the solution, maintaining the temperature at –40 °C in the UV/Vis spectrophotometer. The reaction was followed by recording spectra at intervals of 0.3 s (Figure 6).

X-ray crystallographic analysis

All crystals were handled similarly. The crystals were mounted on a CryoLoop (Hampton Research Corp.) with a layer of light mineral oil and placed in a nitrogen stream at 113(1) K. Measurements were made on a Rigaku R-Axis RAPID/imaging plate area detector, a Rigaku AFC7R/Mercury CCD detector, or a Rigaku AFC11/Pilatus 200 K hybrid pixel array detector with graphite-monochromated Mo_{Kα} (0.71075 Å) radiation. Crystal data and structure refinement parameters are listed in Table S2. The structures of complexes **1–3** were solved by direct methods (SHELXS-97).^[18] The structures were refined on F² by full-matrix least-squares methods using SHELXL-97.^[19] Non-hydrogen atoms were anisotropically refined, except for one *tert*-butyl group in complex **3**, and H atoms were included in the refinement in calculated positions, riding on their carrier atoms. The function minimized was $[\sum w(F_o^2 - F_c^2)^2]$ ($w = 1/[\sigma^2(F_o^2) + (aP)^2 + bP]$), where $P = (\text{Max}(F_o^2, 0) + 2F_c^2)/3$ with $\sigma^2(F_o^2)$ from counting statistics. The functions R1 and wR2 were $(\sum ||F_o| - |F_c||)/\sum |F_o|$ and $[\sum w(F_o^2 - F_c^2)^2/\sum (wF_o^4)]^{1/2}$, respectively. The ORTEP-3 program was used to draw the molecules.^[20]

Acknowledgements

K. M. acknowledges financial support by a Grant-in-Aid for Scientific Research (A) from the Ministry of Education, Culture, Sports, Science, and Technology, Japan. This work is partially supported by CREST (JST), Japan.

Keywords: alcohol oxidation · catalysis · cerium · dioxygen activation · Schiff bases

- [1] a) S. Cotton, *Lanthanide and Actinide Chemistry*, Wiley, Chichester, **2006**; b) N. A. Piro, J. R. Robinson, P. J. Walsh, E. J. Schelter, *Coord. Chem. Rev.* **2014**, *260*, 21.
 [2] a) V. Nair, L. Balagopal, R. Rajan, J. Mathew, *Acc. Chem. Res.* **2004**, *37*, 21; b) K. Binnemans, *Handbook on the Physics and Chemistry of Rare Earths* **2006**, *36*, 281; c) V. Nair, A. Deepthi, *Chem. Rev.* **2007**, *107*, 1862; d) V. Sridharan, J. C. Menendez, *Chem. Rev.* **2010**, *110*, 3805.
 [3] a) Q. Cao, L. M. Dornan, L. Rogan, N. L. Hughes, M. J. Muldoon *Chem. Commun.* **2014**, *50*, 4524; b) P. Gamez, I. W. C. E. Arends, J. Reedijk, R. A. Sheldon, *Chem. Commun.* **2003**, 2414; c) M. F. Semmelhack, C. R.

- Schmid, D. A. Cortés, C. S. Chou, *J. Am. Chem. Soc.* **1984**, *106*, 3374; d) Á. Dijkstra, A. Marino-González, A. M. i Payeras, I. W. C. E. Arends, R. A. Sheldon, *J. Am. Chem. Soc.* **2001**, *123*, 6826; e) J. M. Hoover, S. S. Stahl, *J. Am. Chem. Soc.* **2011**, *133*, 16901; f) W. Yin, C. Chu, Q. Lu, J. Tao, X. Liang, R. Liu, *Adv. Synth. Catal.* **2010**, *352*, 113; g) Y. Jing, J. Jiang, B. Yan, S. Lu, J. Jiao, H. Xue, G. Yang, G. Zheng, *Adv. Synth. Catal.* **2011**, *353*, 1146; h) S. Ma, J. Liu, S. Li, B. Chen, J. Cheng, J. Kuang, Y. Liu, B. Wan, Y. Wang, J. Ye, Q. Yu, W. Yuan, S. Yu, *Adv. Synth. Catal.* **2011**, *353*, 1005.
 [4] a) Y. Hatanaka, T. Imamoto, M. Yokoyama, *Tetrahedron Lett.* **1983**, *24*, 2399; b) S. S. Kim, H. C. Jung, *Synthesis* **2003**, *14*, 2135.
 [5] a) B. L. Ryland, S. D. McCann, T. C. Brunold, S. S. Stahl, *J. Am. Chem. Soc.* **2014**, *136*, 12166; b) E. T. T. Kumpulainen, A. M. P. Koskinen, *Chem. Eur. J.* **2009**, *15*, 10901; c) J. M. Hoover, B. L. Ryland, S. S. Stahl, *J. Am. Chem. Soc.* **2013**, *135*, 2357; d) F. Minisci, F. Recupero, A. Cecchetto, C. Gambarotti, C. Punta, R. Faletti, R. Paganelli, G. F. Pedulli, *Eur. J. Org. Chem.* **2004**, 109.
 [6] a) M. P. Coles, P. B. Hitchcock, A. V. Khvostov, M. F. Lappert, Z. Li, A. V. Protchenko, *Dalton Trans.* **2010**, *39*, 6780; b) G. C. Wang, H. H. Y. Sung, I. D. Williams, W. H. Leung, *Inorg. Chem.* **2012**, *51*, 3640; c) A. Mustapha, J. Reglinski, A. R. Kennedy, *Inorg. Chim. Acta* **2009**, *362*, 1267.
 [7] a) P. Dröse, J. Gottfriedsen, *Z. Anorg. Allg. Chem.* **2008**, *634*, 87; b) A. Vogler, H. Kunkely, *Inorg. Chim. Acta* **2006**, *359*, 4130; c) B. D. Mahoney, N. A. Piro, P. J. Carroll, E. J. Schelter, *Inorg. Chem.* **2013**, *52*, 5970.
 [8] a) E. M. Broderick, P. S. Thuy-Boun, N. Guo, C. S. Vogel, J. Sutter, J. T. Miller, K. Meyer, P. L. Diaconescu, *Inorg. Chem.* **2011**, *50*, 2870; b) J. Gottfriedsen, *Z. Anorg. Allg. Chem.* **2005**, *631*, 2928; c) J. Gottfriedsen, M. Spoida, S. Blaurock, *Z. Anorg. Allg. Chem.* **2008**, *634*, 514.
 [9] a) J.-E. Backvall, *Modern Oxidation Methods*, Wiley-VCH, Weinheim, 2nd ed., **2010**; b) T. Mallat, A. Baiker, *Chem. Rev.* **2004**, *104*, 3037; c) S. S. Stahl, *Angew. Chem. Int. Ed.* **2004**, *43*, 3400; *Angew. Chem.* **2004**, *116*, 3480; d) B. L. Ryland, S. S. Stahl, *Angew. Chem. Int. Ed.* **2014**, *53*, 8824; *Angew. Chem.* **2014**, *126*, 8968; e) S. D. McCann, S. S. Stahl, *Acc. Chem. Res.* **2015**, *48*, 1756.
 [10] a) B. A. Steinhoff, A. E. King, S. S. Stahl, *J. Org. Chem.* **2006**, *71*, 1861; b) A. Dyer, *An Introduction to Zeolite Molecular Sieves*, Wiley, New York, **1988**.
 [11] See the Supporting Information.
 [12] a) T. Saito, H. Nishiyama, H. Tanahashi, K. Kawakita, H. Tsurugi, K. Mashima, *J. Am. Chem. Soc.* **2014**, *136*, 5161; b) T. Yurino, Y. Ueda, Y. Shimizu, S. Tanaka, H. Nishiyama, H. Tsurugi, K. Sato, K. Mashima, *Angew. Chem. Int. Ed.* **2015**, *48*, 14437; *Angew. Chem.* **2015**, *127*, 14645.
 [13] R. Shannon, *Acta Crystallogr. Sect. A* **1976**, *32*, 751.
 [14] a) M. Niemeyer, *Z. Anorg. Allg. Chem.* **2002**, *628*, 647; b) V. Patroniak, M. Kubicki, W. Radecka-Paryzek, *J. Inclusion Phenom. Macrocyclic Chem. Commun.* **2004**, *7*, 455; c) W. Radecka-Paryzek, V. Patroniak, M. Kubicki, *Inorg. Chem. Commun.* **2004**, *7*, 455; d) V. Patroniak, M. Kubicki, A. Mondry, J. Lisowski, W. Radecka-Paryzek, *Dalton Trans.* **2004**, 3295.
 [15] U. J. Williams, D. Schneider, W. L. Dorfner, C. M. Mössmer, P. J. Carroll, R. Anwender, E. J. Schelter, *Dalton Trans.* **2014**, *43*, 16197.
 [16] I. Šalitros, R. Boca, R. Herchel, J. Moncol, I. Nemeč, M. Ruben, F. Renz, *Inorg. Chem.* **2012**, *51*, 12755.
 [17] A. B. Pangborn, M. A. Giardello, R. H. Grubbs, R. K. Rosen, F. J. Timmers, *Organometallics* **1996**, *15*, 1518.
 [18] G. M. Sheldrick, *Acta Crystallogr. Sect. A* **2008**, *64*, 112.
 [19] A. Altomare, M. C. Burla, M. Camalli, G. L. Casciarano, C. Giacovazzo, A. Guagliardi, G. Polidori, *J. Appl. Crystallogr.* **1994**, *27*, 435.
 [20] L. J. Farrugia, *J. Appl. Crystallogr.* **1999**, *32*, 837.

Received: September 24, 2015

Published online on January 21, 2016